Temperature Stability of AgCu Nanoparticles

J. Sopousek[a, b], O. Zobac[a], V. Vykoukal[a], J. Bursik[c], P. Roupcova[c], P. Broz[a, b], J. Pinkas[a, d], and J. Vrestal[c]

[a] Masaryk University, Faculty of Science, Department of Chemistry, Kotlarska 2, 611 37 Brno, Czech Republic, sopousek@mail.muni.cz
[b] Masaryk University, CEITEC MU, Kamenice 5, 62500 Brno, Czech Republic, jan.vrestal@ceitec.muni.cz
[c] Institute of Physics of Materials, ASCR, Zizkova 22, 61662 Brno, Czech Republic, bursik@ipm.cz

ABSTRACT

The Ag-Cu nanoparticles (NPs) were prepared by solvothermal synthesis in colloid state. The colloids were dried in air and heat treated. The individual AgCu NPs and the composite microstructures after heat treatments were investigated by various methods including electron microscopy and high–temperature X-ray powder diffraction (HTXRD). The AgCu randomly mixed, Cu–rich, and Ag–rich face centred cubic (FCC) crystal lattices of particles were detected. The temperature induced sintering was observed experimentally inside HTXRD at 240 °C. The high temperature phase transformations were evaluated by differential scanning calorimetry (DSC). The formation of the silver rich grains during heating under air and evolution of copper oxide microstructures were observed.

Keywords: sintering, microscopy, organometallics, evaporation, DSC, KEMS.

1 INTRODUCTION

There are great differences between the alloys in the conventional (bulk) and nanoparticle forms despite the same chemical composition. Fortunately, these differences offer new space for discovering new innovative nanostructured materials that can be integrated into new technologies. The alloy nanoparticles (nanoalloys) are also targeted by both fundamental and applied research. The high surface-to-volume ratio leads to melting point depression (MPD) of pure metal nanoparticles and alloys. It was predicted theoretically [1] and confirmed experimentally, e.g. [2-7]. Other phase transformation temperatures of nanoalloys change also with respect to bulk alloy. Phase diagrams of nanoalloys respecting the nanoparticle size as an extra variable represent important information on nanostructured materials. Such diagrams can be predicted by CALPHAD approach considering excess surface energy [6], [8-11].

The AgCu stable phase diagram of the bulk alloy represents a simple eutectic system (liquid (L) + Cu-rich FCC phase + Ag-rich FCC phase). The invariant point is 780 °C/Ag–42 at%Cu [12]. The solid Cu_FCC + Ag_FCC equilibrium can be reached also by spinodal decomposition of the metastable FCC AgCu matrix [13].

The predicted eutectic melting point depression (EMPD) of the Ag–Cu eutectic NPs can be observed only if the particles are heated as isolated objects. The individual behavior of NPs can be maintained by stabilization layer (usually organic or oxide) on the nanoparticle surface. The aggregation and sintering processes occur during heating if the stabilization layer is destroyed and metal cores of the AgCu nanoparticles are in touch.

The use of the MPD and EMPD effects of the nanoparticles is considered for lead-free soldering but the sintering process, which can take place at low temperatures also seems very promising. This effect is well known for silver and silver based nanoparticles [14-15].

The surrounding medium has an important influence on the NP reactivity (e.g., the solvent during storage and the gas composition during NP heating). The AgCu NPs behave during heating in inert gas as reported in [13]. The result is completely different in the presence of air during heating as will be reported in this contribution.

2 EXPERIMENTAL

2.1 NPs synthesis

The colloid solutions of the Ag-Cu nanoalloy were prepared by solvothermal co-reduction of silver malonate and copper acetate [9]. The metal weight inputs were equivalent to a particular stoichiometric ratio (metal input equivalent to Ag-42at%Cu in NPs, i.e. eutectic composition). The precursors were dissolved in oleylamine and this solution was injected into a hot dry solvent (230 °C), which consisted of a mixture of oleylamine and octadecene. The reaction was conducted under nitrogen. In the reaction mixture, the metal cations of both metal precursors were reduced at mentioned temperature and the mixture turned to the dark brown colloid solution of the Ag-Cu nanoparticles. The product was separated and purified by repeated precipitation in ethanol, centrifugation, and dispersing in hexane. The particle size was dependent on adherence to thermal conditions of the synthesis.

2.2 Equipment

The hydrodynamic size of the AgCu NPs in hexane was measured by the dynamic light scattering (DLS) method on

a Zetasizer Nano ZS ZEN 3500 instrument (Malvern UK). The metal composition of the AgCu NP samples was obtained by inductively-coupled plasma atomic emission spectroscopy (ICP–OES). The mass of organic residues was also evaluated by difference between the weight of the dry sample and the weight of the analysed metal content.

The metal cores of the NPs were revealed by electron microscopy on a carbon film coated Cu grid. The size and shape of NP cores were investigated using CM12 STEM and JEOL JEM 2100F microscopes with a point resolution of 2.3 Å. The energy dispersive X-ray (EDX) analysis was also used.

The nanoparticles were investigated by high temperature X-ray powder diffraction (HTXRD) on an X´Pert PRO PanAlytical (Netherlands) diffractometer with CoKα radiation. An HTK-16N Anton Paar heating chamber was applied in step mode that enables sample heating (5 K/min) on the platinum strip.

The thermal properties of NPs were evaluated simultaneously by differential scanning calorimetry (DSC), thermogravimetric analysis (TGA) and completed by Knudsen effusion mass spectrometry (KEMS). The experiments were carried out on a Netzsch STA 449 apparatus coupled with Fourier transform infrared (FTIR) spectroscopy under flowing (70 $cm^3 min^{-1}$) synthetic air (20 vol.%) with the heating rate of 10 K min^{-1} and on a Netzsch STA 409 CD/3/403/5/G apparatus equiped with a quadrupole mass spectrometer.

Overall composition and microstructure of the samples after heat treatment were observed by scanning electron microscopy (SEM) using a TESCAN LYRA 3XMU FEG/SEM microscope with an X-Max 80 EDX Oxford Instruments detector.

2.3 Nanoparticle characterization

The freshly synthesized AgCu colloid nanoparticles have an average hydrodynamic size (HS), which involves contributions of the central metal core, surface organic shell and solvation molecules. The metal cores of the AgCu NPs were investigated by TEM. The cores of nanoparticles were of spherical shape and of narrow size distribution. The average core size of the synthesized samples varied from 15 to 30 nm (TEM). The average HS sample sizes (DLS) were from 30 to 50 nm. X–ray powder diffraction detected FCC crystal lattice of the AgCu NPs. The lattice constant (4.084 nm) was smaller than for pure silver. Freshly synthesized samples had no peaks of FCC copper or copper oxides. The metal content (ICP-OES) was (±15 wt%) to eutectic composition.

3 RESULTS

The AgCu colloid nanoparticles were obtained in hexane after synthesis. The simple procedure – drying in air – causes hexane evaporation and formation of composite microstructure visible in **Figure 1**. This samples revealed metallic sheen but they were brittle and electrically non-conductive. The composite involve high portion of organic matter (30–40 wt%).

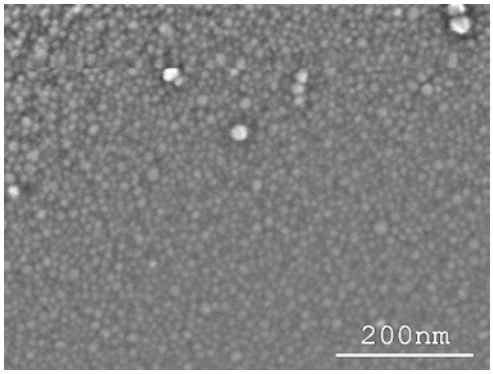

Figure 1: AgCu NPs after drying in air at ambient temperature (SEM).

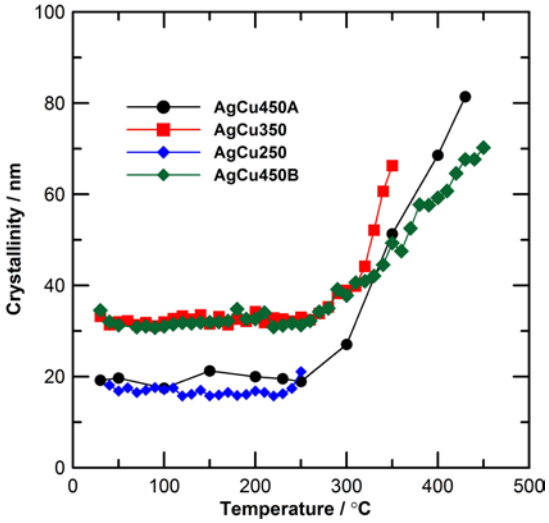

Figure 2: Temperature dependences of crystallinity of the AgCu NP samples if they are heated to 250, 350, and 450 °C (HTXRD).

The dry AgCu NP composite samples were placed on a HTXRD diffractometer under synthetic air, heated (+5 K/min) to programmed temperature, and cooled to ambient temperature. The XRD signal was measured during the heating. The HTXRD pattern computation enabled evaluation of temperature dependences of phase compositions, lattice constants of coexisting phases, crystallinity by Rietveld method, and other data. The changes of the diffraction domain size (crystallinity) are in **Figure 2**. The turn points (240±10) °C on the crystallinity curves show initial temperatures of the metal core sintering.

The example of the final microstructure after heat treatment to 350 °C is in **Figure 3**. The EDX microanalysis revealed large Ag-rich grains (Ag–4wt%Cu) and copper oxide matrix (XRD). The continuous change of surface

microstructure if heated to 450 °C is in **Figure 4**. The samples of the AgCu nanoparticles were also investigated by DSC/TGA methods. The representative signal of the AgCu NP sample (HS = 45 nm, metal content Ag-40.3at%Cu) is in **Figure 5**. The mass loss during the heating was also measured: (70–150) °C/(1–2) wt%, (230–1100) °C/(5–10) wt%. The first mass includes solvent evaporation. Other mass declines are caused by oxygen assisted reactions. The evolution of CO_2 gas was detected by FTIR spectroscopy at 230-250 °C.

Interesting experimental results were also obtained via KEMS during the heating to 1060°C in vacuum ($1 \cdot 10^{-3}$Pa). The AgCu NP composite was decomposed to silver powder (partly contaminated by organic residua) and copper metal, which was deposited outside the inner crucible in Knudsen cell (see **Figure 6**).

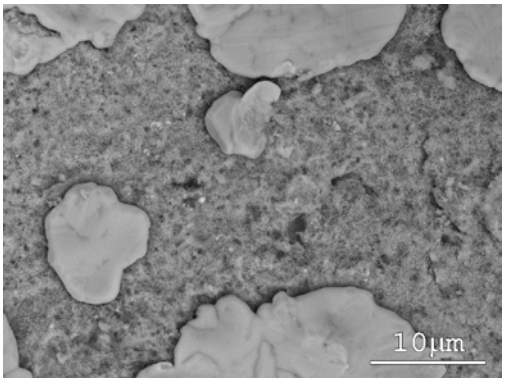

Figure 3: AgCu NPs after heating under air to 350 °C (SEM). Surface microstructure: sintered Ag-rich phase (light grains) and Cu oxide rich (matrix).

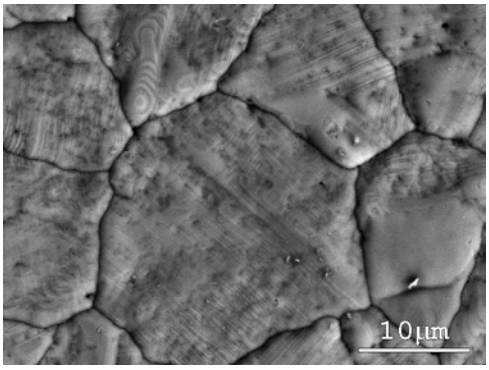

Figure 4: AgCu NPs after heating on air to 450 °C(SEM). Surface microstructure: sintered Ag-rich phase grains only.

4 DISCUSSION

The Ag-Cu randomly mixed NPs were prepared by solvothermal synthesis. The dry AgCu NP samples revealed composite structure (**Figure 1**) with high portion of the organic matter that separated the AgCu NP cores one from another.

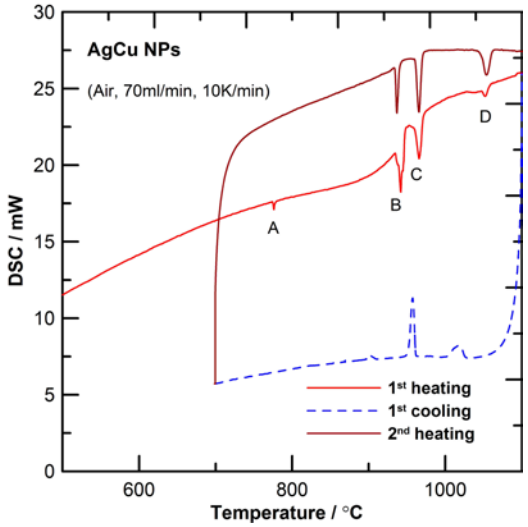

Figure 5: AgCu NPs heating on air to 1100 °C and cycling between 700-1100 °C. Peak onsets: 775 °C (A), 935 °C (B), 961 °C (C), 1042 °C (D). (DSC).

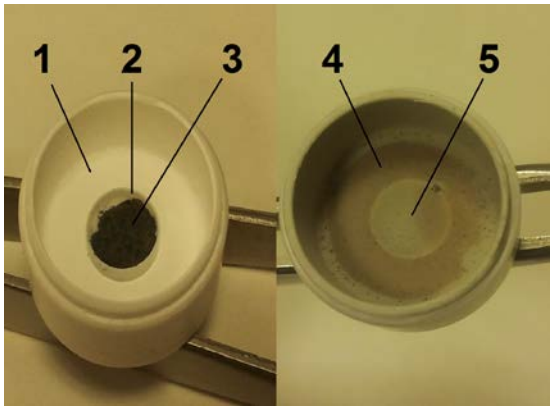

Figure 6: AgCu NP sample before heating to 1060 °C under vacuum in the Knudsen cell (left) and the cell after heating (right). 1…Knudsen alumina crucible, 2…inner alumina crucible, 3 …AgCu NPs, 4 …copper deposit, 5…place after removal of inner crucible.

The stabilizing effect of the organic matter is reduced upon heating the AgCu NPs composite. The sintering of the AgCu NPs starts at (240±10) °C, which little higher than the silver oxide decomposition temperature reported by Hoflund et al. [16]. This leads to hypothesis that sintering is possible only if certain conditions are fulfilled. These conditions may be deoxidation of silver, reaction of stabilizing organic envelope accompanied by the release of carbon dioxide, or their collective action.

The spinodal decomposition of the randomly mixed FCC Ag–Cu lattice to FCC Ag-rich and FCC Cu-rich phase is not allowed under air because the Cu–oxide phase formation is preferred. The Ag–rich phase is separated and

grows up to large grains mainly on surface of the heated sample (**Figure 3**).

The AgCu NP sample evolution under air is completely different from that occurring under vacuum (see **Figure 7**) where the spinodal decomposition and coarsening is observed [13]. Under high vacuum, the copper transport on long distance was observed (see **Figure 6**). The vapour pressure of copper at this temperature range is low and thus the transport effect cannot be explained by deposition from copper gas.

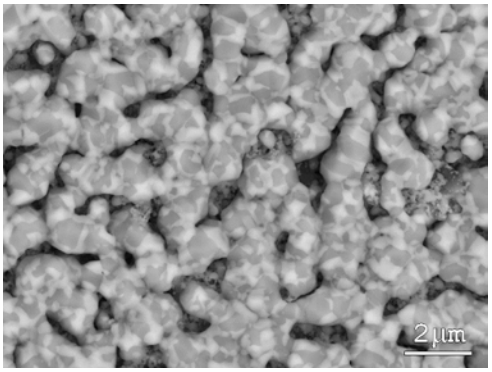

Figure 7: Microstructure of the AgCu NPs after heating (5 K/min) under vacuum to 45 °C and cooling to room temperature (SEM).

The microstructure evolution of the AgCu sample is continued when heated under air above 450 °C. The phase transformations (see **Figure 5**) are detected above 600 °C. The bulk AgCu alloy has the tabulated eutectic temperature of 779.8 °C [12]. Nearly the same temperature 775 °C is assigned to the low peak A at the 1st heating in **Figure 5** and this peak is not present during the 2nd one. It means that the AgCu bulk alloy was transformed under air most likely to Ag–rich phase and copper oxide.

At high temperature region, the peaks B, C, and D were measured (**Figure 5**). The onset temperature of the peak C is 961 °C is equivalent to tabulated liquidus of pure silver. The other peaks (B, D) are difficult to assign because the Ag–Cu–O phase diagram is not well assessed in literature yet.

After heat treatment of the AgCu NPs under air to 1100 °C, the samples consist of silver grains and micro particles of Cu oxides fulfilling the conservation law for Cu and Ag.

5 CONCLUSION

AgCu colloids having the AgCu randomly mixed FCC cores were prepared by solvothermal synthesis and characterized. The colloids were dried under air. The samples were objects of the heat treating experiments. The special effects were measured by high temperature XRD, TEM, SEM, and by thermal analysis and following events can be proposed:

100-150 °C – Evaporation of solvent traces. 150–230 °C – Destabilization of the organic layer, penetration of oxygen to metal surface and formation of thin oxide layer.
(240±10) °C – AgCu NPs decomposition to Ag-rich phase and Cu oxide particles and starting Ag-rich phase sintering.
600-960 °C – Completion of burning of organic residues.
960 °C - Melting of silver grains at presence of Cu oxide.

Acknowledgement. Financial support of the Czech Science Foundation of Czech Republic for the project "Stability and phase equilibria of bimetallic nanoparticles" (GA14-12653S) is gratefully acknowledged as well as of the CEITEC-MU (CZ.1.05/1.1.00/02.0068).

REFERENCES

[1] J. Lee, J. Park, and T. Tanaka, CALPHAD 33, 377, 2009.
[2] P. Buffat and J.-P. Borel, Phys. Rev. A 13, 2287, 1976.
[3] Y. H. Jo, I. Jung, C. S. Choi, I. Kim, and H. M. Lee, Nanotechnology 22, 225701, 2011.
[4] J. F. Sánchez-Ramírez, U. Pal, L. Nolasco-Hernández, J. Mendoza-Álvarez, and J. A. Pescador-Rojas, J. of Nanomaterials, 1, 2008.
[5] S. Tabatabaei, A. Kumar, H. Ardebili, P. J. Loos, and P. M. Ajayan, Microelectronics Reliability 52, 2685, 2012.
[6] J. Sopousek, J. Vrestal, A. Zemanova, and J. Bursik, J. of Mining and Metallurgy B48, 419, 2012.
[7] K. Sim and J. Lee, J. of Alloys and Compounds 590, 140, 2014.
[8] J. Sopousek, J. Vrestal, J. Pinkas, P. Broz, J. Bursik, A. Styskalik, D. Skoda, O. Zobac, and J. Lee, CALPHAD 45, 33, 2014.
[9] J. Sopousek, J. Pinkas, P. Broz, J. Bursík, V. Vykoukal, D. Skoda, A. Styskalik, O. Zobac, J. Vrestal, A. Hrdlicka, and J. Simbera, J. of Nanomaterials, 1, 2014.
[10] J. Park, J. Lee: Phase diagram reassessment of Ag–Au system in cluding size effect, CALPHAD, vol.32, no. 1, pp.135–141, 2008.
[11] G. Kaptay, J. of Mater. Sci. 47, 8320, 2012.
[12] A. Dinsdale, A. Watson, A. Kroupa, J. Vrestal, A. Zemanova, and J. Vizdal, "Atlas of Phase Diagrams for Lead/Free Soldering", COST 531, vol.1, 2009.
[13] J. Sopousek, O. Zobac, J. Bursik, P. Roupcova, P. Broz, J. Pinkas, and J. Vrestal, Heat-induced spinodal decomposition of AgCu nanoparticles, Phys. Chem. and Chem. Phys., 2015, under review.
[14] J. G. Bai, Z. Z. Zhang, J. N. Calata, and G.-Q. Lu, IEEE Transactions on Components and Packaging Technologies 29, 2006.
[15] J. Sopousek, J. Bursik, J. Zalesak, and Z. Pesina, J. Mining and Metallurgy B48, 63, 2012.
[16] G. Hoflund, Z. Hazos, and G. Salaita, Phys. Rev. B62, 11126, 2000.